HELIUM UCN SOURCE AT THE EXTRACTED BEAM OF THERMAL NEUTRONS

E.V. Lychagin[1], A.Yu. Muzychka[1], G.V. Nekhaev[1], V.V. Nesvizhevsky[2], E.I. Sharapov[1] and A.V. Strelkov[1]

[1] *Joint Institute for Nuclear Research, Dubna, Russia*
[2] *Institute Max von Laue – Paul Langevin, Grenoble, France*

Abstract

We propose a new method for production of ultracold neutrons (UCNs) in superfluid helium. The principal idea of the method consists of installing a helium UCN source into an external beam of thermal or cold neutrons and in surrounding this source with a solid methane moderator/reflector cooled down to the temperature of ~4 K. The moderator/reflector plays the role of an external source of cold neutrons, which are needed to produce UCNs. The flux of accumulated cold neutrons could exceed the flux of incident thermal or cold neutrons due to their numerous reflections from methane; also the source size could be significantly larger than the incident beam diameter.

We provide preliminary calculations of cooling of neutrons in a cavity inside solid methane. These calculations show that such a source of UCNs, being installed at an intense source of thermal or cold neutrons like the ILL reactor in Grenoble, the PIK reactor in Gatchina or the ESS spallation source in Lund, could provide the UCN density of the order of 10^5 cm^{-3}, while the production rate would be of the order of 10^7 UCN/s^{-1}.

Main advantages of such a UCN source include its low radiative and thermal load, relatively low cost and convenient accessibility for any maintenance work.

We have carried out an experiment on cooling of thermal neutrons in a methane cavity with the wall temperature of 6.6 K. The experimental data confirm the results of our calculations of the spectrum and flux of neutrons in the methane cavity.

Introduction

Further progress in the field of studies with ultracold neutrons (UCNs) [1, 2], as a tool for nuclear and particle physics [3, 4, 5], is often limited by available UCN densities. Therefore many projects of new advanced UCN sources are pursued in various scientific centers in the world; they are aiming to increase the available UCN densities and fluxes by at least 1-2 orders of magnitude.

The principle of production of UCNs in superfluid helium was proposed already in 1975 in ref. [6]. It is based on the fact that a neutron could excite a phonon with the energy of 1.02 meV in liquid ^{4}He. If the energy of incident neutron exceeds slightly this value (1.02 meV) the neutron will be scattered to the UCN energy. UCNs could be produced via this mechanism only from incident cold neutrons with energies from a very narrow range as the UCN energy is as small as <300 neV. A neutron could also excite two or more phonons in helium simultaneously. The cross section of such multi-phonon scattering is lower by several orders of magnitude than the cross section of one-phonon scattering. However the total energy of exited phonons could be found within a much broader energy range, and thus UCNs could be produced in a multi-phonon process from a much broader energy range of incident neutrons. Therefore both these process would give comparable contributions to the UCN production provided that the initial cold neutron spectrum is broad.

It was also shown in the cited work that the produced UCNs could be stored in superfluid helium for a long time if the helium temperature is ~ 1K or lower. This fact allows building up the UCN density in a source of this type up to very high values.

Helium UCN sources, as well as solid-deuterium UCN sources, seem to be most promising at present. There are several projects of helium UCN sources in the stage of their realization or design [7, 8, 9, 10, 11]. A drawback of helium sources as compared to solid-deuterium sources consists of very low temperatures needed in order to provide long UCN lifetimes in superfluid ^{4}He: thus the lifetime drops down from 10^4 s to 1 s if the temperature increases from 0.6 K to 2 K [12, 13]. Advantages of helium sources consist of the transparency of the physical processes involved, of the relatively low cost and the possibility to install them outside of a reactor/spallation source zone.

The concept of UCN sources at external beams of thermal neutrons

It was noted in ref. [14] in 1998 that if a UCN source filled in with liquid helium at the temperature of below 1 K is installed in a beam of cold neutrons surrounded with a cold neutron reflector (i.e. the reflector provides a trap for cold neutrons used to produce UCNs) then one could noticeably increase the flux of cold neutrons in the source and thus increase the UCN generation rate. Beryllium oxide and Plexiglas at a temperature of several degrees were considered as possible materials for the reflector. The mean path of cold neutrons in the source of a cylindrical or spherical shape could increase by the factors 2.2 and 2.5 accordingly. This idea has not been realized as such gains could be achieved only in relatively small volumes. The reason is in the fact that the angular distribution of reflected neutrons is isotropic in contrast to the initial narrow angular distribution. Thus one could not use a section of a neutron guide (with the length several times larger than the width) for such a source; the path of cold neutrons in a guide-shaped source (and thus the generation rate) would be higher anyway than in a spherical source of equal volume.

However if we replace the reflector material by another one providing simultaneously good moderation and reflection properties then one could 1) considerably increase the flux of cold neutrons in the source and thus its production rate, and also 2) use “cheap” and intense thermal neutrons instead of “expensive” and less intense cold neutrons for UCN production [15]. In fact such a moderator/reflector plays the role of a cold neutron source. Thus the maximum flux density in beams of cold neutrons at the ILL reactor reaches ~ 10^{10} cm^{-2}s^{-1}, while the maximum flux density of thermal neutrons at the same reactor could reach ~ 10^{11} cm^{-2}s^{-1} as shown below.

Such an UCN source is shown schematically in Fig. 1; it is surrounded with a moderator/reflector, which plays the role of an external cold neutron source. The moderator/reflector in the figure surrounds also the input neutron guide in order to avoid leakages of neutrons (from the trap) with the angular divergence exceeding the narrow angular divergence in the initial neutron beam. The larger the albedo of the reflector is, the higher the saturated neutron flux density in the source is; in the limit of the reflector albedo equal unity, the neutron flux density accumulated in the cavity is strictly equal to the neutron flux density in the thermal neutron source. For the PIK and ILL reactors it would be equal to ~10^{15} n·cm^{-2}s^{-1}.

A matter with maximum albedo for cold neutrons, which we have found, is solid methane in the phase II at the temperature of ~ 4 K (we leave aside composite materials based on nanoparticle reflectors [16, 17, 18], which we are analyzing currently in view of even further increase in the attainable albedo). On one hand, albedo of methane is slightly higher than albedo of reflectors considered in ref. [14]. On another hand, solid methane is simultaneously one of the best cold moderators. This latter property of methane is due to the

fact that it is a molecular crystal with a very round molecule; thus it provides rather flexible rotational degrees of freedom even at very low temperatures.

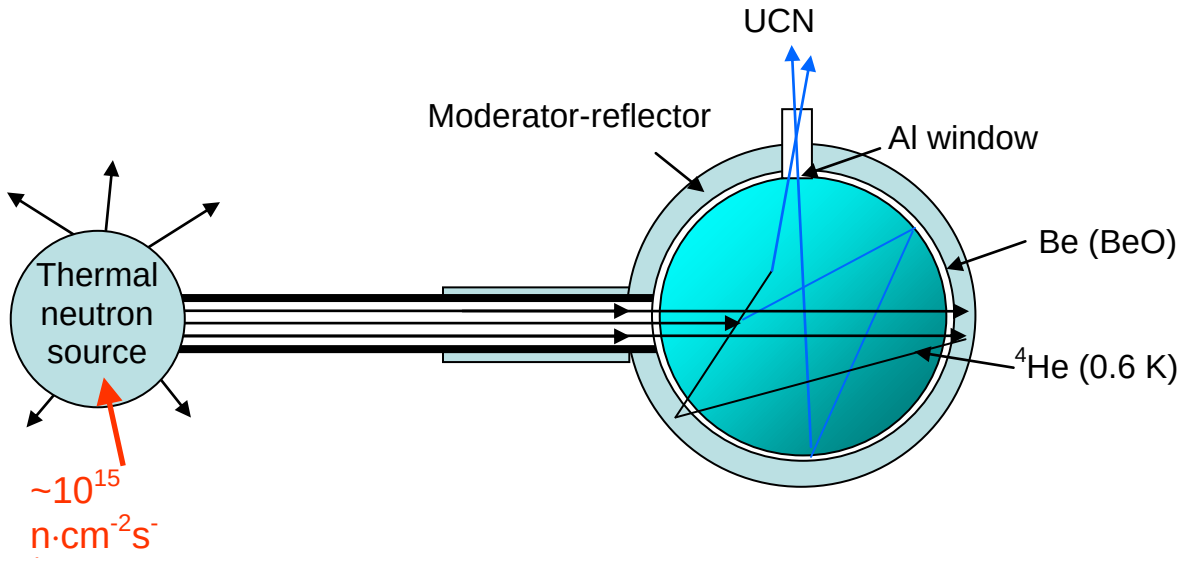

Fig. 1. A scheme of an UCN source surrounded by a moderator/reflector

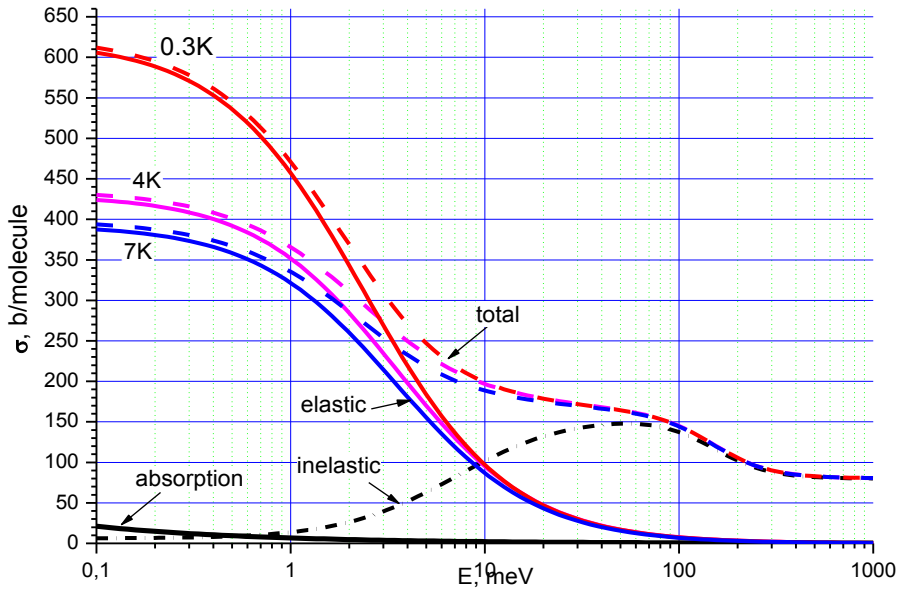

Fig. 2. The cross section of neutron scattering normalized to one molecule of solid methane (CH_4) in the phase II at different temperatures is shown as a function of neutron energy.

Solid grey lines correspond to the cross sections of elastic scattering at respective temperatures. Black dashed-dotted line indicates the cross section of inelastic scattering. Grey dashed lines show the total scattering cross section at a given temperature. Black solid line gives the absorption cross section.

Another particularity of solid methane is parallel alignment of spins of hydrogen atoms in the methane molecule at low temperatures. The scattering of low energy neutrons becomes coherent for one molecule and stays incoherent for different molecules. Therefore there is no optical potential for neutrons of low energy as there is for materials with coherent scattering, and the cross section increases with decreasing the neutron energy. Cross sections of neutron scattering in solid methane at different temperatures are presented in Fig. 2 as a function of neutron energy; the data are taken from refs. [19, 20].

Estimation of thermal neutron flux density in a neutron guide

Before calculating parameters of the proposed UCN source, we estimate the flux of thermal neutrons, which could be achieved in an external neutron guide of existing neutron sources.

The most intense worldwide steady neutron source is currently the ILL reactor; it provides the thermal neutron flux density of $J_0 = 1.2 \cdot 10^{15}$ n/(cm^2 s) in the vicinity of its active zone. The distance from its active zone to the outside surface of its biological shielding is about 4 m. There are holes with the maximum diameter of 20 cm in the biological shielding of the reactor for the installation of neutron guides. It is realistic to install an UCN source at the end of a neutron guide with the diameter of 20 cm at the distance of 5 m from the center of the reactor active zone.

So, let us assume that there is a cylindrical tube with the length of L = 5 m and the diameter of D = 20 cm (the square area cross section is thus S=314 cm^2). Let us assume also that one end of the tube is an isotropic source of thermal neutrons with the flux density equal $J_0 = 1.2 \cdot 10^{15}$ n/(cm^2 s). Then the neutron flux density through the opposite end of the tube is:

$$J = J_0 \frac{S}{4\pi L^2} = J_0 \cdot 10^{-4} = 1.2 \cdot 10^{11} \text{ n/(cm}^2 \text{ s).} \quad (1)$$

The integral flux will be equal:

$$F = 3.8 \cdot 10^{13} \text{ n/s.} \quad (2)$$

Note that the real neutron flux could be about twice larger due to the radiation of neutrons through side walls of the tube and reflection of neutrons from the biological shielding.

Note also that the flux density is proportional to the square of the tube diameter, and the integral flux is proportional to the 4-th power of the diameter.

Modeling of neutron spectrum in the solid methane cavity

We have simulated the spectrum of neutrons accumulated in a solid methane cavity. The simulation was carried out using the program *MCNP-4C* [21] with a special kernel for solid methane; the kernel was used in refs. [20, 22] and was kindly provided to us by the authors.

As a result of this model calculation we established the optimum parameters of moderator/reflector. We found that the optimum thickness of methane is ~3 cm; an increase in its thickness does not increase noticeably the number of neutrons in the cavity. The optimum temperature of methane is ~4 K; a decrease in the temperature also does not increase the number of neutrons in the cavity. The optimum diameter of the cavity is 40 – 50 cm if the input neutron guide diameter is 20 cm.

Figs. 3 and 4 show spectra of neutrons accumulated in a spherical cavity with the internal diameter of 40 cm surrounded with solid methane. Here Φ is the neutron fluence

averaged over the cavity volume per one incident neutron. The velocity distribution of incident neutrons is Maxwellian with the temperature of 300 K; they enter the cavity through the input guide with the diameter of 20 cm.

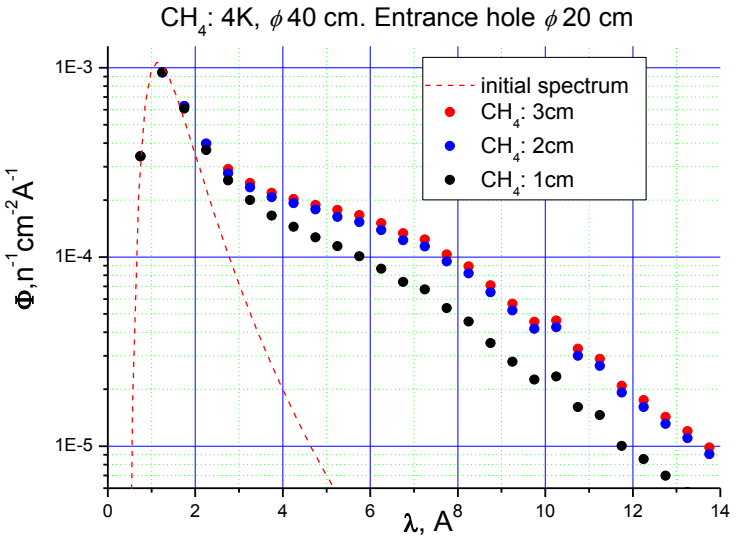

Fig. 3. Mean neutron fluence in a spherical cavity with the diameter of 40 cm surrounded with solid methane at the temperature of 4 K is shown as a function of neutron wavelength. Line indicates the mean fluence of incident neutrons with the temperature of 300 K normalized per 1 neutron. Points show the mean fluence of accumulated neutrons, normalized per 1 incident neutron, for different thickness of the cavity walls equal to 1, 2 and 3 cm.

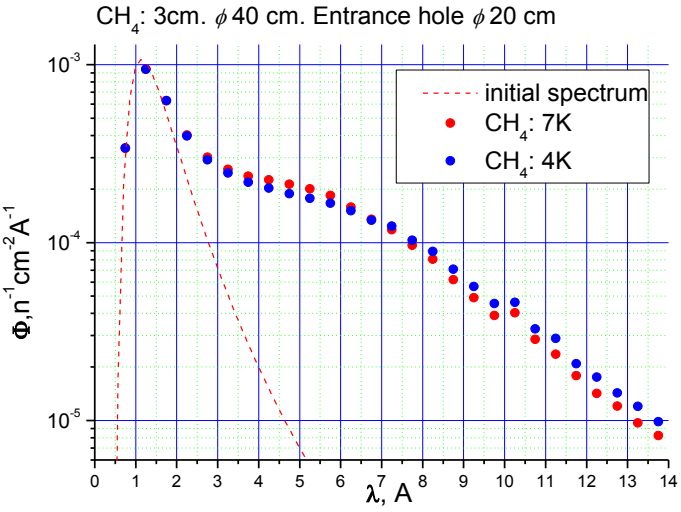

Fig. 4. Mean fluence in a spherical cavity with the diameter of 40 cm surrounded with solid methane walls with the thickness of 3 cm. Line indicates the mean fluence of incident neutrons with the temperature of 300 K normalized per 1 neutron. Points show the mean fluence of accumulated neutrons, normalized per 1 incident neutron, for different temperatures of methane equal to 7 K and 4 K.

Estimation of the generation rate in the source

For one-phonon processes only and for the UCN energy below the beryllium optical potential, the UCN generation rate in liquid helium [23] equals:

$$R_1 = 4.55 \cdot 10^{-8}\ dJ/d\lambda\ (8.9\ Å)\ cm^{-3}\ s^{-1}\ . \qquad (3)$$

For the input flux (2), a spherical cavity with the diameter of 40 cm and the mean fluence $d\Phi/d\lambda\ (8.9\ Å) = 6.7 \cdot 10^{-5}\ n/(cm^2\ Å)$, (see Figs. 3, 4) one could get:

$$dJ/d\lambda\ (8.9\ Å) = 2.5 \cdot 10^{9}\ n/(cm^2\ s\ Å) \quad \text{and} \quad R_1 = 116\ n/(cm^3\ s). \qquad (4)$$

Estimations of UCN production due to multi-phonon processes differ in different works. Thus for the spectra of accumulated neutrons as shown in Figs. 3-4, multi-phonon processes could contribute with a factor of increase in the UCN production rate equal to a value ranging from 1.25 to 3.5 [24, 25]. Thus the lower estimation of the UCN production rate is: $R = 145\ n/(cm^3\ s)$.

The total number of UCNs produced in the source per second is $5 \cdot 10^6$ UCN/s.

One could propose the following characteristics of the source: the number of UCNs produced in the source per one incident thermal neutron is $1.3 \cdot 10^{-7}$ UCN/s/n.

For the coefficient of loss of UCNs in the walls of the UCN accumulation volume equal $\eta = 10^{-4}$, the mean partial storage time of UCNs related to wall losses is $\tau_w \approx 450$ s; with account for the neutron β-decay lifetime the storage time will be equal $\tau \approx 300$ s.

Preliminary estimations indicate that the thermal heat to the source with the diameter of 40 cm will raise to ~0.2 W for the input neutron flux (2); at such a heat load the source could be cooled down to the temperature of 0.6 K.

If the helium temperature is 0.8 K, the UCN storage time in helium is equal to the neutron β-decay lifetime. If the helium temperature is 0.6 K, it is a factor of 10 larger and thus such losses even could be neglected.

Thus, the maximum UCN density in the source is:

$$n_{UCN} = R \cdot \tau = 4.4 \cdot 10^4\ UCN/cm^3. \qquad (5)$$

We have given the lower estimate for the UCN production rate in the source. The upper estimation would be a factor of ~ 5 larger.

These estimations are valid for a source with the diameter of 40 cm and the neutron guide diameter of 20 cm. If the source diameter is 30 cm, the UCN density would practically stay the same because the leakage of 8.9 Å-"parent neutrons" through the input neutron guide will increase. On the other hand, the total number of produced UCNs ("children") would decrease by a factor of ~ 2. An increase of the source size will increase the production rate proportionally to the diameter value; however it will decrease the UCN density proportional to the reciprocal diameter square.

Measurements

In order to verify validity of the calculations presented in Figs. 3 and 4, we have measured the spectra and intensities of neutrons accumulated in a solid methane cavity.

The measurements were performed using the instrument DIN-2PI [26] at the reactor IBR-2 [27] (JINR, Dubna). The instrument was designed to measure inelastic scattering of neutrons using the time-of-flight method. The length of the input arm of DIN-2PI is 20 m; it is measured between the reactor and a sample, which scatters neutrons (a cryostat with solid methane in our case). The output arm length is 7 m; it is measured between the sample and the detectors. Choppers are installed in the input arm of the spectrometer; they select a mono-line with the wavelength (time-of-flight) resolution of ~1%.

A scheme of measurement is shown in Fig. 5.

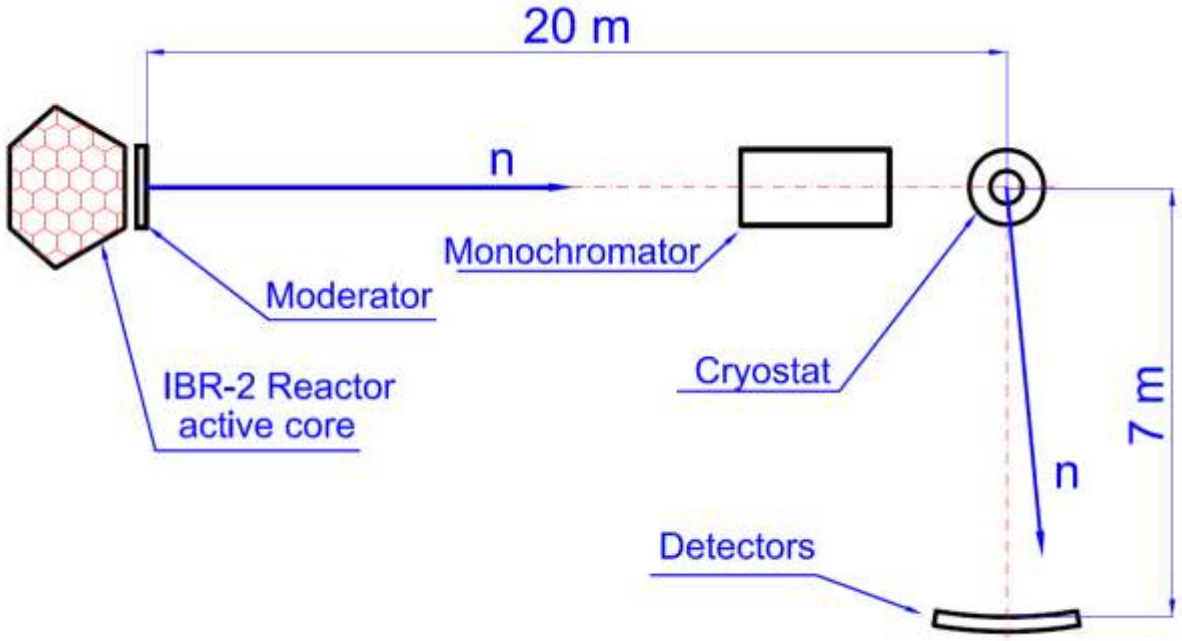

Fig. 5. A scheme of measurement of the spectra and intensities of neutrons accumulated in a methane cavity performed with the instrument DIN-2PI.

A sample of solid methane with a cylindrical cavity measuring 12 x 12 cm with the wall thickness of 3 cm was grown in the cryostat. The temperature of methane was slightly different in different points of the sample within the range from 6 K to 7.2 K. The temperature was stable in time. Two holes were left in the walls of methane cavity, one for the neutron entrance and another one for their exit, at the angle of 90° relative to each other. The square area of every hole was equal to ~ 7 cm^2. The cryostat was surrounded with Cd-shielding so that thermal neutrons could enter into the cryostat only through the entrance window, and they could escape from the cavity to the detectors only through the exit window. Before escaping into the detector, neutrons had to have two or more reflections from the cavity walls.

Results of the measurements

We selected only one mono-line of incident thermal neutrons with the energy of 25.0 meV (1.81 Å). There were also many "background" fast and epithermal neutrons (that could pass through a cadmium sheet) in the initial beam. A major fraction of these neutrons could be separated using the time-of-flight technique. However some faster neutrons could penetrate into the cryostat, scatter in methane and escape to the detector during the same time intervals as neutrons from the initial thermal mono-line do. To exclude an influence of fast neutrons, we measured the so-called cadmium difference, i.e. the difference of the count rate with the input beam open and the count rate with a sheet of cadmium in the input beam, which totally absorbed the initial thermal beam. Fig. 6 shows the results of these measurements.

The difference of these measurements allows calculating the spectrum of neutrons thermalized in methane.

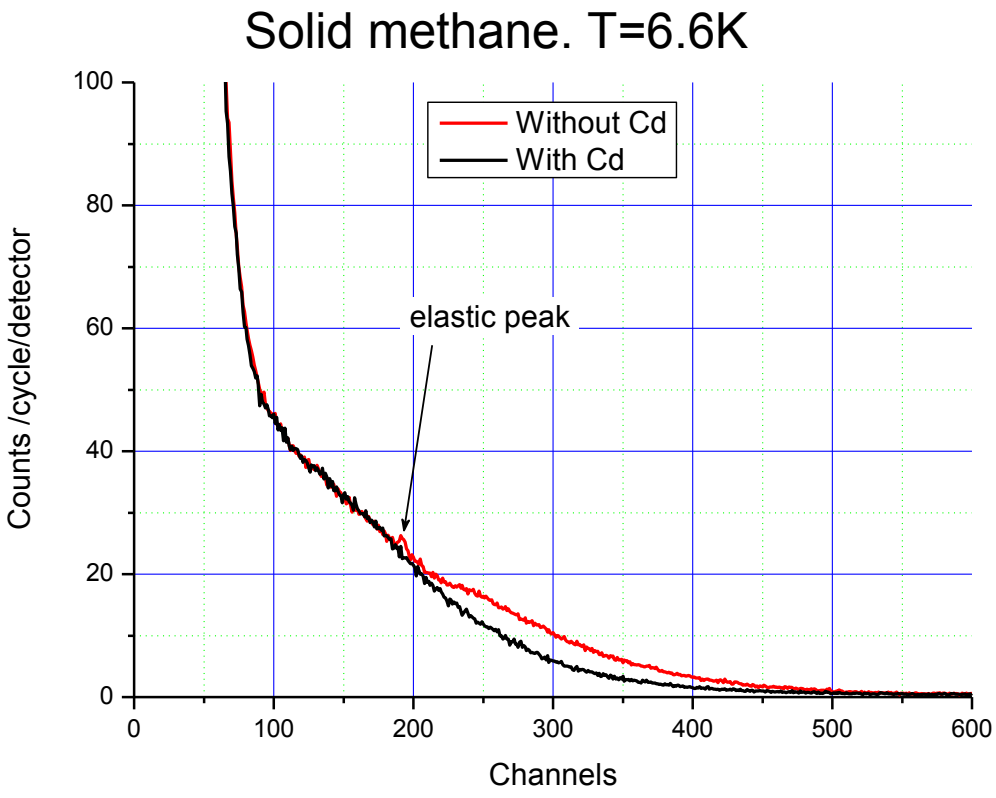

Fig. 6. Count rate in the detector as a function of the time interval after a reactor pulse. Results of measurements with the initial beam open are shown with gray line. Results of measurements with a sheet of cadmium in the incident neutron beam are indicated with black line. The width of one time channel is 64 μs.

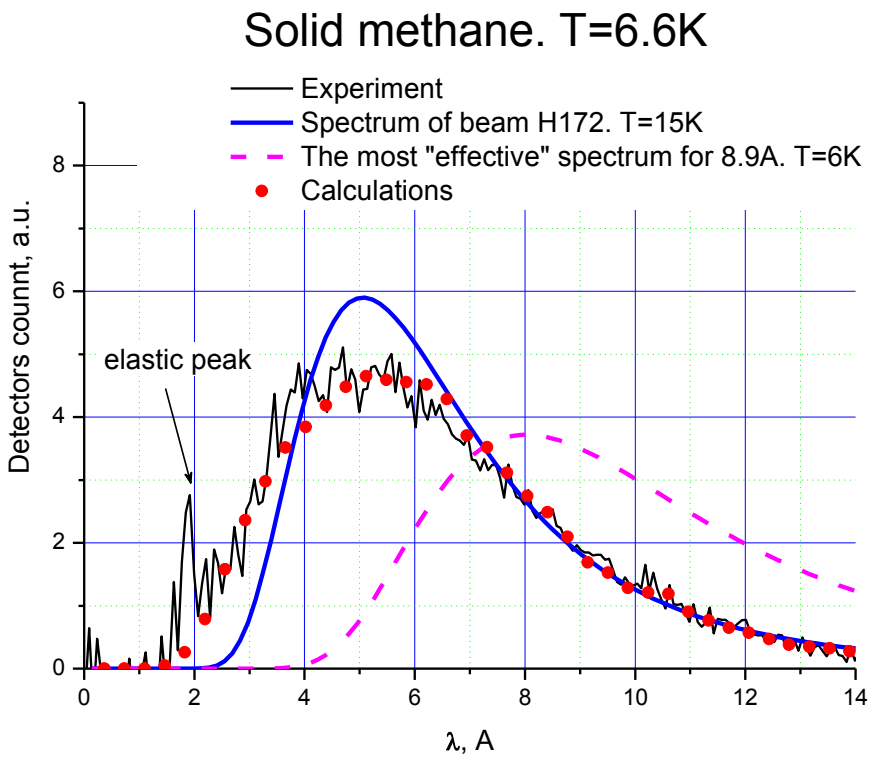

Fig. 7. Spectrum of neutrons escaping from the methane cavity through the exit window: Thin line indicates the results of measurements. Points correspond to the numerical simulation of our experiment. Dashed line illustrates the Maxwellian distribution, which provides the largest count rate of neutrons with the wavelength of 8.9 Å. Blue line shows a Maxwellian distribution fitting the data in the best way. The integrals under all curves are equal to each other.

Fig. 7 presents the results of measurements of the spectrum of neutrons escaping from the methane cavity through the exit window. We performed a numerical simulation of our experiment using the same computer MCNP-4C code as used for the source simulation. The numerical simulation almost ideally coincides with the measurements, except for one feature, which is not important in this case. Namely, one clearly observes measured extra neutrons, which did not change their energy during their storage in the cavity – the elastic peak. We do not reproduce this peak in simulations.

Also we show Maxwellian spectra in Fig. 7 for comparing them with the measured results. One spectrum provides the maximum number of neutrons with the wavelength of 8.9 Å (our "ideal" spectrum). Another one provides a shape closest to the measured data. This latter spectrum is also very close to cold neutron spectra in beams at the ILL. The integrals under all spectra are equal to each other.

As an additional verification of validity of simulations of neutron fluxes accumulated in the methane cavity, we performed an analogous measurement with methane replaced with distillated water at the temperature of 292 K. In this test, the number of initial neutrons entering the cryostat was the same, and the spectrum was the same, as in measurements with methane. Results of this measurement are shown in Fig. 8.

The initial spectrum, as mentioned above, is a monoline with the wavelength width smaller than 1%. Such a width could not be shown graphically in the scale in Figure 8 (the "elastic peak" in Figures 6 and 7 has larger width as it is washed out due to time-of-flight spread caused by some delay of neutrons in the methane cavity).

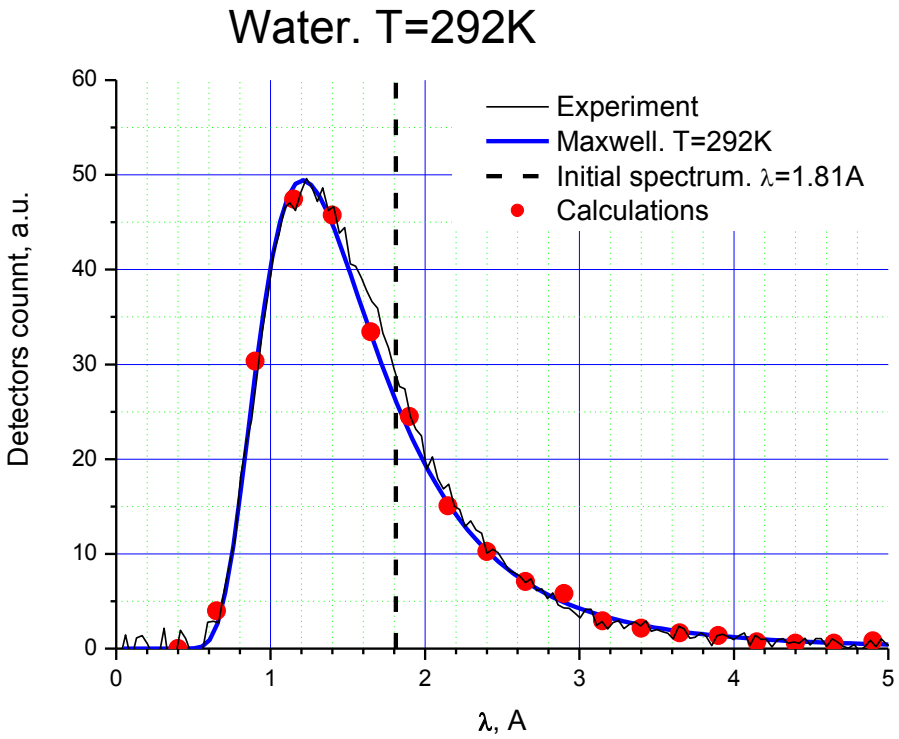

Fig. 8. The spectrum of neutrons escaping from the water cavity through the exit window is shown as a function of neutron wavelength. Thin line indicates the measured results. Points correspond to the results of numerical simulations of this experiment. Blue line indicates the Maxwellian distribution for the temperature equal to 292 K.

As clear from this figure, the results of numerical simulations perfectly agree with the measured data. Also the ratios of integrals under the spectra for water and methane agree for results of simulations and measurements:

Experiment: $$\frac{\int N_{\text{det}}^{H_2O}(\lambda)d\lambda}{\int N_{\text{det}}^{CH_4}(\lambda)d\lambda} = 2.01 \pm 0.02 \qquad (6)$$

Simulation: $$\frac{\int N_{\text{det}}^{H_2O}(\lambda)d\lambda}{\int N_{\text{det}}^{CH_4}(\lambda)d\lambda} = 1.94 \pm 0.04 \qquad (7)$$

Here $N_{\text{det}}^{H_2O}$ is the count rate for water at the temperature of 292 K and $N_{\text{det}}^{CH_4}$ is the count rate for methane at the temperature of 6.6 K.

All these performed measurements demonstrated high accuracy of simulations both in terms of absolute values of neutron fluxes accumulated in a methane cavity and also in terms

of spectra of accumulated neutrons. Accordingly, we confirm all simulated characteristics of the UCN source. On the other hand, one should underline that now we could provide rather precise estimations of these characteristics basing these estimations solely on the measured data, even without simulations.

In fact, if we know the value of albedo of thermal neutrons from water then the relation (6) and a know geometry of the cavity (see above) allow calculating the albedo from solid methane.

MCNP simulations of neutron albedo from water at the temperature of 292 K, for normal incidence of neutrons with the energy of 25 meV, provides the value: 0.787±0.008. Nearly the same value could be obtained for isotropic incidence of neutrons with the Maxwellian distribution with the temperature of 292 K: 0.806±0.008. Thus, in all cases typical for experiments, the albedo from water is about 0.8. Taking into account that we observe in experiments the neutrons after their second and further reflections from the cavity walls, and also taking into account the sizes of entrance and exit holes and relation (6), we get albedo from methane equal 0.65. Assuming the spectrum of neutrons in the methane cavity is the same as that shown in Fig. 7, one could calculate the neutron flux in a methane cavity of any geometry, and thus the UCN production rate in the source.

The characteristics of the UCN source estimated in this way are higher by ~ 20% than those given above that means a very good accuracy. The main reason for this deviation consists of the fact that the neutron energy after their first reflection from a methane cavity wall is higher than their energy after consequent reflections, and the contribution of such neutrons into the total neutron flux is more important (as the number of neutrons decreases after each reflection).

The measured spectrum (Fig. 7) is compared with the simulated spectrum inside the cavity (Figs. 3-4) in Fig. 9. For convenience of normalization, we excluded from the simulated spectrum inside the cavity a contribution of neutrons from the initial beam; they marginally affect the UCN production.

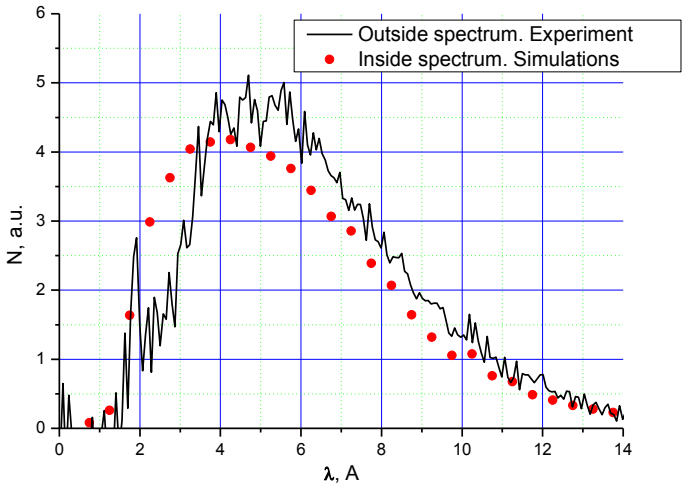

Fig. 9. The neutron spectrum inside the methane cavity and the spectrum of neutrons escaping through the exit hole are compared. Thin line indicates results of measurements outside of the cavity. Points correspond to the numerical simulation of the spectrum inside the cavity.

Conclusion

Our calculations showed that the installation of a helium UCN source in an external beam of thermal neutrons at the ILL reactor in Grenoble, at the PIK reactor in Gatchina or at the ESS spallation source in Lund would allow achieving the UCN density of ~10^5 UCN cm^{-3}. The production rate of such a UCN source is ~ 10^7 UCN·s^{-1}. Our measurements confirmed validity of these calculations.

The main source of thermal load in such a source, if it is installed at a heavy-water reactor like that at the ILL for instance, consists of gamma-quanta produced in the capture of neutrons in the moderator/reflector itself. Preliminary calculations of the thermal load to the source show that one could even considerably increase the flux of incoming neutrons, and thus one could increase the density and the flux of UCNs in the source. For instance, an increase of the diameter of the input neutron guide from 20 cm to 30 cm would increase the input neutron flux by a factor of ~5. However, one should take into account that an increase of the heat load over 1 – 2 W would complicate cooling of liquid helium in the source below the required temperature of 0.8 K. Therefore the limit of production rate in such a source is probably close to ~10^8 n·s^{-1}.

On the one hand, the proposed UCN source provides parameters much better than those of existing UCN sources; in particular the UCN density would be a factor of 103 higher. Onthe other hand, its parameters are similar to those inmost optimistic alternative projects while the price is much lower.

Acknowledgement

We are sincerely grateful to the staff of the DIN 2PI instrument, in particular to V.I. Morozov for their help during this experiment.

Also we are sincerely grateful to Y. Shin, C. M. Lavelle, W. Mike Snow, David V. Baxter, Xin Tong, Haiyang Yan and Mark Leuschner for providing us the program for calculations of the interaction of neutrons with cold methane as well as to V.A. Artemiev, E.P. Shabalin and R. Golub for useful discussions.

References

1 Ya.B. Zeldovich, *JETP* **9**, 1389 (1959)
2 V.I. Luschikov et al, *JETP Lett.* **9**, 23 (1969)
3 J. Butterworth et al, *Nucl. Instr. Meth. A* **440**, V (2000)
4 V.V. Nesvizhevsky et al, *Nucl. Instr. Meth. A* **611**, VII (2009)
5 I. Antoniadis et al, *Compt. Rend. Phys.* **12**, 703 (2011)
6 R. Golub and J.M. Pendlebury, *Phys. Lett. A* **53**, 133 (1975)
7 Ph. Schmidt-Wellenburg et al, *Nucl. Instr. Meth. A* **611**, 267 (2009)
8 Y. Masuda et al, *Phys. Rev. Lett.* **89**, 284801 (2002)
9 G. Greene et al, *J. Res. NIST* **110**, 149 (2005)
10 http://nuclear.uwinnipeg.ca/ucn/triumf/post-acot-5-26-8/ucn-post-acot-may08.pdf
11 A.P. Serebrov et al, Phys. Sol. St. **52**, 1034 (2010)
12 R. Golub et al, *Z. Phys. B* **51**, 187 (1983)
13 Y. Abe1 and N. Morishima, *Nucl. Instr. Meth. A* **463**, 293 (2001)
14 P.D. Bangert et al, *Nucl. Instr. Meth. A* **410**, 264 (1998)
15 S. Baessler et al, *Compt. Rend. Phys.* **12**, 729 (2011)
16 V.V. Nesvizhevsky et al, *Nucl. Instr. Meth. A* **595**, 631 (2008)

17 E.V. Lychagin et al, *Phys. Lett. B* **679**, 186 (2009)
18 V.V. Nesvizhevsky, *Phys. At. Nucl.* **65**, 400 (2002)
19 S. Grieger et al, *J. Chem. Phys.* **109**, 8 (1998)
20 Y. Shin et al, *Nucl. Instr. Meth. A* **620**, 382 (2010)
21 J.F. Briesmeister, Ed.MCNP^{TM} - A general Monte Carlo N-particle transport code, version 4C, LA-13709-M (Los Alamos National Laboratory, Los Alamos, 2000).
22 Y. Shin et al, *Nucl. Instr. Meth. A* **620**, 375 (2010)
23 C.A. Baker et al, *Phys. Lett. A* **308**, 67 (2003)
24 E. Korobkina et al, *Phys. Lett. A* **301**, 462 (2002)
25 Ph. Schmidt-Wellenburg et al, *Nucl. Instr. Meth. A* **611**, 259 (2009)
26 I.V. Kalinin et al, *Tech. Phys.* **59**, 307 (2014)
27 Yu.G. Dragunov et al, *At. En.* **113**, 1 (2012)